PROCEEDINGS OF SPIE

SPIEDigitalLibrary.org/conference-proceedings-of-spie

Characterization of a compact 6-band multifunctional camera based on patterned spectral filters in the focal plane

H. E. Torkildsen, H. Hovland, T. Opsahl, T. V. Haavardsholm, S. Nicolas, et al.

SPIE.

Characterization of a compact 6-band multifunctional camera based on patterned spectral filters in the focal plane

H. E. Torkildsen, H. Hovland, T. Opsahl, T. V. Haavardsholm, S. Nicolas, T. Skauli*
Norwegian Defence Research Establishment (FFI), P. O. Box 25, NO-2027 Kjeller, Norway

ABSTRACT

In some applications of multi- or hyperspectral imaging, it is important to have a compact sensor. The most compact spectral imaging sensors are based on spectral filtering in the focal plane. For hyperspectral imaging, it has been proposed to use a "linearly variable" bandpass filter in the focal plane, combined with scanning of the field of view. As the image of a given object in the scene moves across the field of view, it is observed through parts of the filter with varying center wavelength, and a complete spectrum can be assembled. However if the radiance received from the object varies with viewing angle, or with time, then the reconstructed spectrum will be distorted. We describe a camera design where this hyperspectral functionality is traded for multispectral imaging with better spectral integrity. Spectral distortion is minimized by using a patterned filter with 6 bands arranged close together, so that a scene object is seen by each spectral band in rapid succession and with minimal change in viewing angle. The set of 6 bands is repeated 4 times so that the spectral data can be checked for internal consistency. Still the total extent of the filter in the scan direction is small. Therefore the remainder of the image sensor can be used for conventional imaging with potential for using motion tracking and 3D reconstruction to support the spectral imaging function. We show detailed characterization of the point spread function of the camera, demonstrating the importance of such characterization as a basis for image reconstruction. A simplified image reconstruction based on feature-based image coregistration is shown to yield reasonable results. Elimination of spectral artifacts due to scene motion is demonstrated.

Keywords: Multispectral imaging, Hyperspectral imaging, Coregistration, Misregistration, Georeferencing, Multiband filters

1. INTRODUCTION

Multi- and hyperspectral imaging is being used in an ever expanding range of applications employing a wide variety of concepts for image formation. Hyperspectral imaging is attractive for its ability to capture the full spectral information in the incoming light. On the other hand, hyperspectral imagers tend to suffer from low light throughput, for dispersive or filter-based instruments, or image reconstruction processes prone to artifacts, for interferometric instruments. Generally, hyperspectral imagers tend to be complex and bulky, and hence relatively expensive. Multispectral imagers may have better light throughput, and can potentially be more compact and affordable.

Multispectral imagers come in a large number of forms beyond conventional RGB color cameras, for example filter wheel cameras and beamsplitter-based cameras with multiple image sensors. Notably, there is no single camera concept which is clearly preferable over others. This is true both for multi- and hyperspectral imaging, and many new concepts are being explored, see for example [1-6]. For applications requiring compact and low cost spectral imaging, a few camera concepts stand out by requiring only a single imaging lens and a single image sensor with no moving parts. Of these, the concepts based on scanning of the scene are well suited for use on small airborne platforms, where the platform movement provides scanning. An example is the "linear variable filter" concept [7]. However with non-simultaneous sampling of different spectral components there is a risk of spectral artifacts if the scene properties vary during the scanning of a given point, for example due to parallax or movement.

We have developed a multispectral camera concept employing patterned bandpass filters which seeks to minimize spectral artifacts [8]. As illustrated in Fig. 1, bandpass filters are laid out in a pattern of stripes across the scan direction so that a given point in the imaged scene will be observed through each filter in turn. Then a spectral image can be assembled by combining data from multiple image frames. An important feature is that the filter pattern provides sampling of all bands multiple times in an interspersed order, which enables various strategies for consistency checking in the image reconstruction. To minimize artifacts due to parallax and other angular and temporal dependencies, the total

* E-mail: torbjorn.skauli@ffi.no

Algorithms and Technologies for Multispectral, Hyperspectral, and Ultraspectral Imagery XX,
edited by Miguel Velez-Reyes, Fred A. Kruse, Proc. of SPIE Vol. 9088, 908819 · © 2014
SPIE · CCC code: 0277-786X/14/$18 · doi: 10.1117/12.2054477

extent of filters should be as small as possible in the scanning direction. This leaves most of the image sensor area available for conventional 2D imaging, resulting in a multifunctional camera along similar lines as in Ref. [9]. The concept is discussed in some more detail in [8].

As a basis for the reconstruction of a spectral image, the camera needs to be accurately characterized with respect to radiometric, geometrical and spectral properties. Some aspects of the camera performance need characterization to a higher level of detail compared to customary characterization of cameras. In particular, it is important to achieve the best possible spatial coregistration of different bands to preserve spectral integrity [10,11]. Therefore it is of interest to characterize the point spread function (PSF) instead of the modulation transfer function (MTF). With knowledge of the PSF, it will eventually be possible to adapt the image reconstruction to make a controlled compromise between spatial resolution and spectral integrity [12].

In this paper we present results from characterization of a demonstrator camera, with emphasis on a technique for measuring the two-dimensional shape of the PSF and its variation with wavelength. It is also shown how spectral artifacts due to scene movement can be mitigated thanks to the repeated sampling pattern.

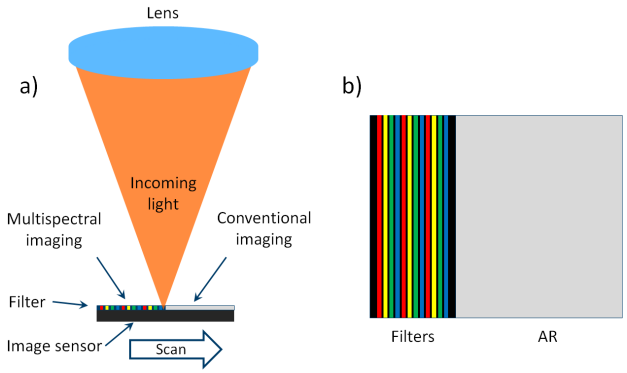

Figure 1. a) Illustration of the multispectral imaging concept. A patterned multiband filter is placed on an image sensor behind an imaging lens. The camera is scanned relative to the scene. b) Sketch of filter layout. The filters for different bands are laid out in stripes across the scan direction. An important feature is that the bands are repeated multiple times along the scan. This enables reconstruction of an image with improved spectral integrity. The remaining part of the filter substrate area is antireflection coated to allow for conventional 2D imaging in most of the field of view.

2. MULTISPECTRAL CAMERA

To test the multispectral imaging concept, we have built a demonstrator based on an AVT GE1650 camera employing a Truesense KAI-2020 CCD image sensor with 1600x1200 pixels and 7.4 µm pixel pitch. The camera is used with a Zeiss Planar ZF IR-corrected lens with 85 mm focal length and aperture setting F/4. A 6-band patterned filter is mounted on the image sensor. The filter is held in place by a mechanical clamp and spacers underneath to form an air gap of about 20 µm between the filters and the CCD. The spectral response of all 6 bands at normal incidence is shown in Fig. 2 together with the actual filter layout. Each individual filter area is shaped as a stripe across the image sensor. Filters in front of the lens block light outside the range 450 to 900 nm. In operation, the camera is scanned across the scene in a direction perpendicular to the stripe pattern. The filter stripes are about 10 pixels wide, separated by shadow masks to minimize crosstalk between bands. For the imaging experiments shown here, we use a rotary stage to scan the camera across an outdoor scene.

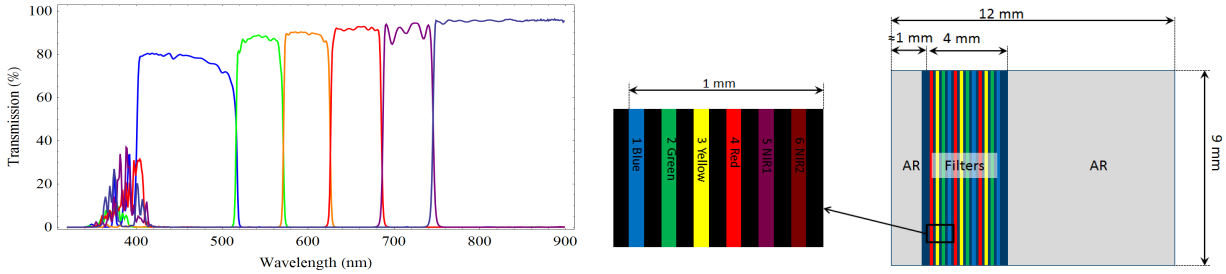

Figure 2. Details of the patterned filter. Left: Measured transmission spectra for each of the six bands. Right: Actual layout of the filter in the demonstrator camera, with 4 repeats of 6 bands and AR-coated regions on both sides of the filter.

3. MEASUREMENT OF POINT SPREAD FUNCTION

In our context, the resolution of a camera is described by the PSF, understood here as the two-dimensional spatial distribution of responsivity for a detector element in the image sensor. The PSF may have a relatively strong variation with wavelength, depending mainly on the properties of the lens. The spectral dependence of the PSF can be controlled in the lens design, but achieving a wavelength-independent PSF is nontrivial. (Mirror objectives are less wavelength dependent, but present their own set of problems and challenges.) When a commercial lens is used, such as for our demonstrator, the specifications given by lens manufacturers invariably leave many questions unanswered, including that of the spectral dependence of lens PSF. In any case, it is useful to be able to characterize the PSF experimentally. We have therefore established a procedure for direct measurement of the full PSF based on the method outlined in Ref. [11].

The measurement setup is illustrated in Fig. 3. The camera is focused on an illuminated slit 10 μm wide, located 3.4 m away. (For simplicity, no collimator is used.) The slit width corresponds to 0.03 pixels in the image. The slit is translated in subpixel steps across several pixels in the field of view. For each step, several image frames are recorded and averaged. By collecting the readings for a single pixel within the scan area, we get a direct measurement of the projected PSF in a direction orthogonal to the slit, apart from a known small amount of broadening due to the finite width of the slit. As an example, Fig. 4 shows the projected PSF in one direction for all bands. By using a rotary stage, the scanning of the slit is repeated in a set of 48 directions equally spaced around the circle, so that each PSF projection is recorded in opposing directions. By rotating the camera to a new orientation, the image of the slit is moved to characterize different parts of the field of view, most importantly the different regions of the filter. The setup is motorized, including the camera rotation, and the measurement is fully automated.

To reconstruct the 2D PSF, it is necessary to know the position of the translation where the slit intersects the axis of the rotation stage. This can be determined from the data. Since the slit is symmetrical, the projected PSFs recorded in opposing directions should be flipped copies of each other if the flipping is centered on the rotation axis. Thus by determining the relative offset of the pair of curves (from their centroids, after flipping one of them), we can estimate the position in the scan where the slit intersects the axis. This estimation can be repeated for each pair of opposing scans, allowing us to check for inconsistencies due to mechanical imperfections. For our current setup we find that the center position inconsistency is within 60 μm in the slit plane, demagnified to 1.5 μm in the focal plane, or 20% of the pixel pitch. Though not completely negligible, the inconsistencies due to mechanical imperfection are sufficiently small to record good data, as demonstrated by the results below. For each pair of opposing scans, both PSF projections are resampled to their common center position and their average is used in the reconstruction.

The 2D PSF is reconstructed from the 24 resampled PSF projections using the inverse Radon transform as described in Ref. [13]. For every projection, each frequency component of the Fourier transform is multiplied with the absolute value of their frequency, except the DC value which is multiplied by ¼. A moving average filter is convolved with the result, and the inverse Fourier transform is applied. The result is then back projected along the scan line in image space, and the PSF is the sum of all 24 back projections normalized so that the integrated volume under the PSF is unity.

From a single set of image data, it is possible to reconstruct PSFs for several pixels in a neighborhood in the field of view. Figure 5 shows overlaid PSFs of four pixels in the well-focused band 613-642 nm. The figure also shows the summation of these PSFs, indicating residual variations that might be due to non-ideal fill factor of the image sensor. Figure 6 shows measured PSF for each of the six bands and for the unfiltered panchromatic region of the image sensor. Here the focus has been set to optimize the sharpness of the panchromatic image. There are very clear differences in the sharpness of focus between different bands, with a particularly large broadening for the longest wavelengths.

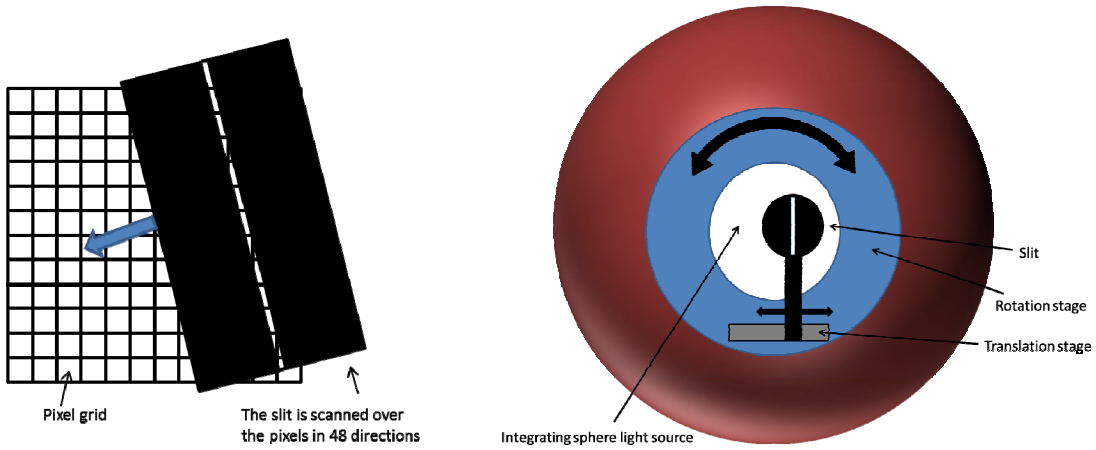

Figure 3. Setup for measuring PSF. Left: measurement principle. An illuminated slit is scanned across the field of view in several directions. Each scan determines the projection of pixel PSF in one direction. From the set of PSFs projected in different directions, the two-dimensional PSF can be estimated by tomographic reconstruction. Right: scanning slit source setup. An integrating sphere with halogen lamp source illuminates a 10 µm wide slit. The multiband camera with F=85mm lens is viewing the slit from a distance of about 3.4 m. The slit is stepped in subpixel increments over a distance of several pixels using a translation stage. The translation stage is mounted on a rotation stage, and the scan is repeated in a set of different directions.

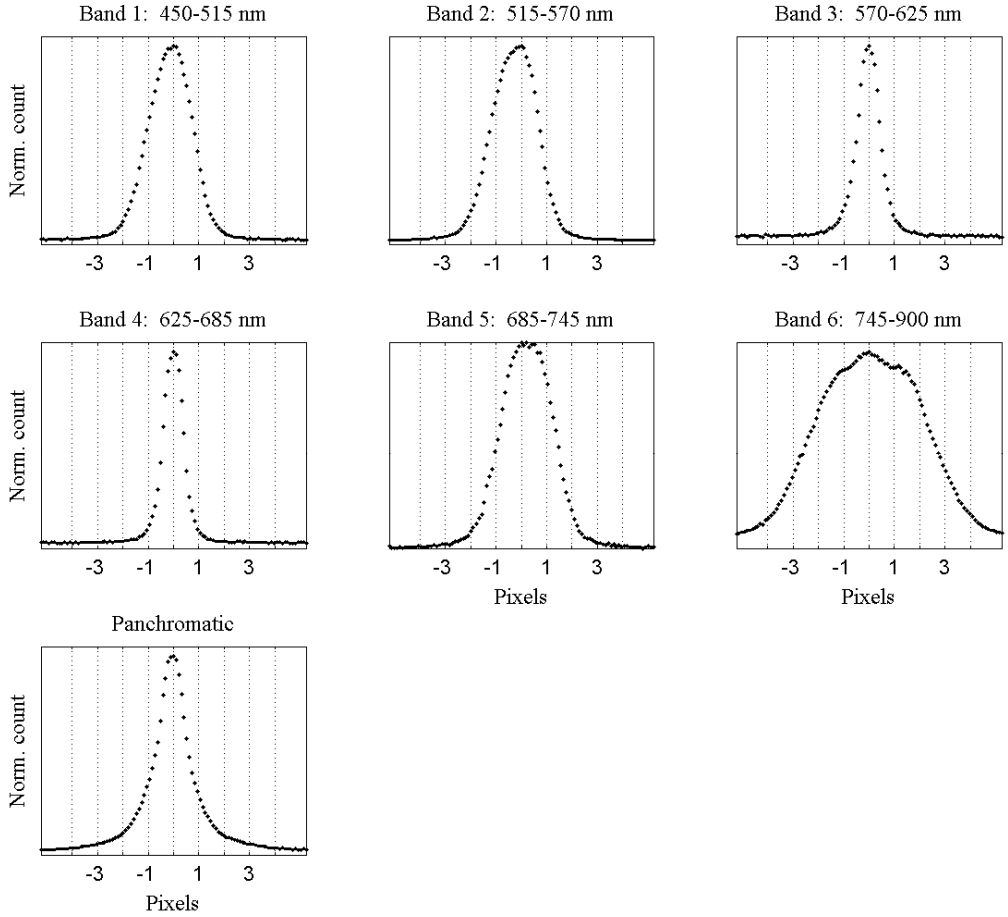

Figure 4. Example recorded data from scanning the slit across single pixels in each of the six bands, as well as an unfiltered panchromatic pixel. The Ordinate is normalized pixel signal value, and the abscissa is the relative slit position.

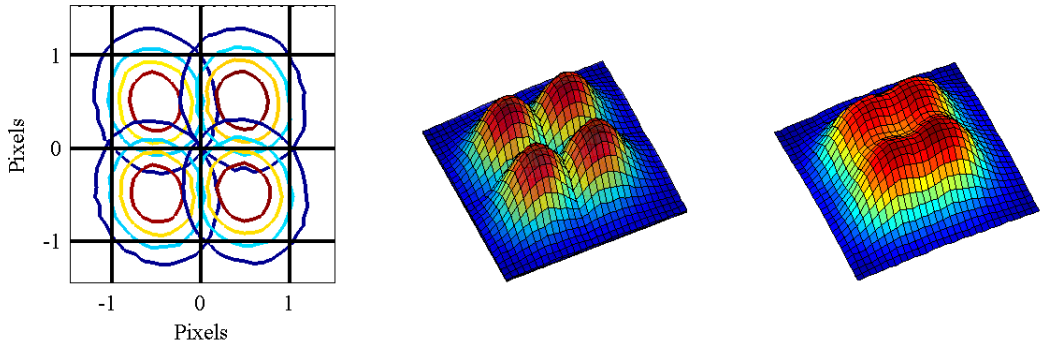

Figure 5. Left: Reconstructed 2D PSF for four neighboring pixels in the spectral band 613-642 nm. The contour lines are at 20, 40, 60 and 80 percent of the maximum value of each PSF. Middle: 3D plot of the same four neighboring pixels. Rights: Result of summation of the four PSFs.

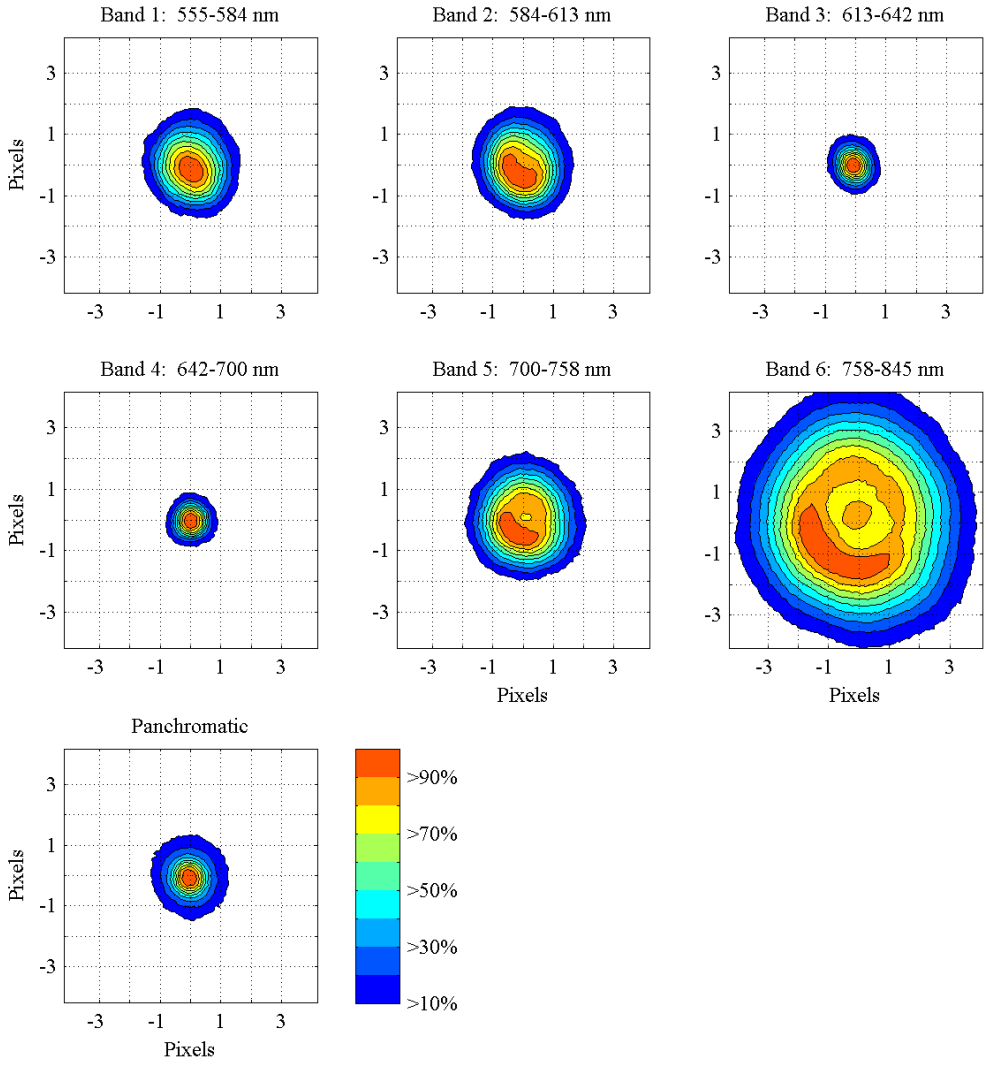

Figure 6. Contour plots of measured PSF for pixels in each of the six bands, taken from one set of neighboring filter stripes. Also shown is the PSF for a pixel in the unfiltered area. Contours and colors represent PSF amplitude relative to the peak value. Amplitudes below 10% are not shown. The noise level is a few percent of the peak value.

Based on the data in Fig. 6 we can calculate values for the coregistration metric proposed in Ref. [11], taking into account any post-processing of the data in the formation of an output image. In the simplest possible case, an output pixel is composed from one pixel reading in each of the spectral bands, centered on the same point in the scene. The spectral variation of PSF is then as shown in Fig. 6, and we can calculate the coregistration error directly from the measured data. Table 1 shows the resulting matrix of coregistration error metrics between band pairs. In the integral to form the metric value, we omit regions were both PSFs are below 5% of their peak value, to limit the influence of noise. The largest coregistration error is then 0.79, between bands 4 and 6. Thus in a worst case, the pixel is centered on a target whose size is approximately equal to the PSF width of band 4, and band 6 will observe a target-to-background contrast which is reduced by 79% from the correct value. Clearly, the measurement of PSF becomes an essential basis for design of an optimized image reconstruction method in a given application. We also observe that the measurement setup can be seen as a tool for measuring the wavelength-dependent PSF of lenses, an interesting capability in itself.

Table 1. Coregistration error metric values for all pairs of bands determined from the measured PSF, representing a simplistic image reconstruction where an output pixel spectrum is formed from one input pixel in each band, see text.

	Band 1	Band 2	Band 3	Band 4	Band 5	Band 6
Band 1	0.00					
Band 2	0.16	0.00				
Band 3	0.20	0.34	0.00			
Band 4	0.25	0.41	0.09	0.00		
Band 5	0.21	0.12	0.43	0.49	0.00	
Band 6	0.50	0.58	0.73	0.79	0.51	0.00

4. PRELIMINARY IMAGE RECONSTRUCTION RESULTS

A sequence of images was captured by scanning a snowy urban scene with the camera mounted on a rotary stage. A single raw image frame is shown in Fig. 7. The filters are clearly seen as a darker region with vertical black stripes from the shadow masks. The scene was mainly static during the scan, apart from some passing cars. One of the passing cars can be seen in the filter region of Fig. 7.

Based on accurate estimates of the camera pose for all images, the spectral information from individual images can be projected into a common image plane chosen for the multispectral image. Due to the design, points in the scene will be sampled several times for each spectral band, and care has to be taken in order to exploit this information and produce the best possible multispectral image.

Figure 7. A single image from the demonstrator camera. The region with clearly visible vertical stripes is caused by the filter mounted directly in front of the detector array. The dark regions at the top and bottom of the image are due to the clamp holding the filter. The foreground car in the filter region is moving through the scene faster than the scan, potentially causing spectral artifacts.

Figure 8. A reference image of the scene produced by coregistering the unfiltered region of several images from the scan.

Figure 9. Four RGB images of the scene produced by combining spectral information from different filter stripes sampling the red, green and blue spectral bands. Spectral artifacts due to a passing car are clearly seen in the lower right part.

Figure 10. The RGB representation of the spectrally reconstructed multispectral image of the scene.

Here we show results of a preliminary image reconstruction chain using feature based image registration [8,14]. A reference image, shown in Fig. 8, was created by coregistering the unfiltered image regions from a subset of the recorded image frames. By registering all individual images with this reference image, the spectral information from different filter stripes was mapped into 24 separate band images. Combining images for the red, green and blue spectral bands for each of the four filter sets, we obtain four separate RGB images of the scene as illustrated in Fig. 9. These images exhibit strong spectral artifacts due to motion in the scene: A passing car has been sampled at different times by the filter stripes, leaving three imprints in each image. The repeated sampling of each band allows us to eliminate this motion-induced artifact from the image. Here we form the final six-band image of the scene by adopting a simplistic strategy where each spectral band in an output pixel is the median of the four sub-images for the band. This effectively removes the passing car from the image, as illustrated by the final RGB image in Fig. 10.

As shown above, the PSF shape varies strongly over the spectral range. In the reconstructed images this can be seen as a wavelength-dependent blur consistent with the measured PSF in the different bands. Figure 11. shows a small section of the scene in each band as it was reconstructed for 6 neighboring filter stripes. A good six-band image can only be constructed at a reduced resolution. It can be observed that in this particular case a 5-band image could be reconstructed at higher resolution while maintaining a given degree of coregistration.

Figure 11. A small region of the scene as it was reconstructed in six band images. On the top row, from left to right, are the band images for 555-584nm, 584-613nm and 613-642nm. On the bottom row, from left to right, are the band images for 642-700nm, 700-758nm and 758-845nm.

5. DISCUSSION AND CONCLUSIONS

Spectral imagers based on filtering in the focal plane come in a variety of forms and have potential for being very compact. It is clear from the outset, though, that image reconstruction may be very demanding. To ensure good coregistration between spectral bands, the resolution of the output image will have to be lower than the resolution of raw images, unless PSF shape and scanning is controlled extremely tightly. To find a compromise between resolution and coregistration in the output image, it is necessary to know the properties of the optics in detail. The results here, from a high-end NIR-corrected lens, show large differences in the image sharpness between different bands. If an output pixel is formed by individual pixel values from the original images, the focus differences would lead to large coregistration errors even if the input pixels are centered on the same point in the scene. Based on the measured PSF shape, an optimized reconstruction strategy can be formulated for a given application, given details about scanning and scene geometry.

We observe that the method for measuring wavelength-dependent PSF of a lens is an interesting capability in itself. Such detailed information is rarely provided for commercial lenses or cameras. We speculate that at this level of detail there may be significant differences between commercially available spectral imagers that are not apparent from their specifications.

The camera concept shown here can compensate for some types of imperfections in the recording, as illustrated by the elimination of a moving object from the stationary scene in Fig. 10. Still, accurate positioning of the recorded pixels is critical for the spectral reconstruction. The rotational scan used here is an easy case, and fair results have been demonstrated from a simplistic image reconstruction. For less well controlled scan motions, such as on a moving platform over scenes with 3D topography, the problem of spectral image reconstruction is significantly more challenging. Many tools are available to handle this problem, such as navigation sensors, image-based navigation and 3D reconstruction. Therefore there is reason to believe that a good image reconstruction performance can be achieved, enabling very compact filter-based multispectral imagers with good spectral integrity.

REFERENCES

[1] Bodkin, A., Sheinis, A., Norton, A., Daly, J., Beaven, S., Weinheimer, J.," Snapshot Hyperspectral Imaging – the Hyperpixel Array Camera," Proc. SPIE 7334, 73340H (2009)

[2] Gao, L., Kester, R. T., Tkaczyk, T. S., "Compact Image Slicing Spectrometer (ISS) for hyperspectral fluorescence microscopy," Opt. Expr. 17, 12293 (2009)

[3] Cavanaugh, D. B., Lorenz, J. M., Unwin, N., Dombrowski, M., "VNIR hypersensor camera system," Proc. SPIE 7457, 74570O (2009)

[4] Tack, N., Lambrechts, A., Soussan, P., Haspeslagh, L., "A Compact, High-speed and Low-cost Hyperspectral Imager," Proc. SPIE 8266, 82660Q (2012)

[5] Høye, G., Fridman, A., "Mixel camera - a new push-broom camera concept for high spatial resolution keystone-free hyperspectral imaging," Opt. expr. 21, 11057 (2013)

[6] Ferrec, Y., Taboury, J., Sauer, H., Chavel, P., Fournet, P., Coudrain, C., Deschamps, J., Primot, J., "Experimental results from an airborne static Fourier transform imaging spectrometer," Appl. Opt. 50, 5894 (2011)

[7] Mika, A. M., "Linear-wedge spectrometer," Proc. SPIE 1298, 127–131 (1990)

[8] Skauli, T., Torkildsen, H. E., Nicolas, S., Opsahl, T., Haavardsholm, T., Kåsen, I., Rognmo, A., " A compact camera for multispectral and conventional imaging based on patterned filters," Appl. Opt. in press (2014)

[9] Delauré, B., Michiels, B., Biesemans, J., Livens, S., Van Achteren, T., "The geospectral camera: A compact and geometrically precise hyperspectral and high spatial resolution imager," International Archives of the Photogrammetry, Remote Sensing and Spatial Information Sciences, Volume XL-1/W1, ISPRS Hannover Workshop 2013, 21 – 24 May 2013, Hannover, Germany

[10] Mouroulis, P., Green, R. O., Chrien, T. G., "Design of pushbroom imaging spectrometers for optimum recovery of spectroscopic and spatial information," Appl. Opt. 39(13), 2210–2220 (2000)

[11] Skauli, T., "An upper-bound metric for characterizing spectral and spatial coregistration errors in spectral imaging," Opt. Expr. 20, 918-933 (2012)

[12] Skauli, T., " Information capacity as a figure of merit for spectral imagers: the trade-off between resolution and coregistration," Appl. Opt. 52, C58

[13] Hovland, H., "Tomographic scanning imager," Opt. Expr. 17, 11371-11387 (2009)

[14] Harley, R., Zisserman, A., [Multiple View Geometry in computer vison], Cambridge University Press (2003)